RACE-T Experimental Activities
A Complete Overview of the Different Subcritical Measurement Techniques

Roberto Rosa

ENEA, Via Anguillarese, 301, 00060 Roma, Italy, roberto.rosa@casaccia.enea.it

Mario Carta (ENEA)
Gorge R. Imel (ANL)
Christian Jammes (CEA)
Stefano Monti (ENEA)

In the period between February 2004 – February 2006, in view of the past TRADE project and the subsequent RACE experiment planned in the frame of the EUROTRANS Integrated Program of the 6th European Framework Program, different experimental activities were carried out in the 1 MW TRIGA reactor operated by ENEA in his Casaccia Research Center near Rome. In that time the reactor operation was mainly in sub-critical conditions, with the exception of the critical reference core assessment at the beginning of the campaign where the maximum power was 50 W. The RACE-T campaign includes fission rate measurements (performed with a special instrumented fuel element,) investigation of different sub-critical configurations (with D/T generator in the core center,) and development of special devoted instrumentation and acquisition systems. The main outcomes of the intense experimental campaign will be illustrated.

I. INTRODUCTION

The objective of the European Integrated Project EUROTRANS[1] of the EURATOM 6th Framework Program is to bring answers to the high level nuclear waste transmutation in ADS. The EUROTRANS experimental activities have been grouped into the ECATS domain, namely Experiment on the Coupling of an Accelerator, a spallation Target and a Subcritical blanket.

The RACE-T experiment, formerly named TRADE[2], is part of ECATS. The European experimental teams performing the different experiments operated in the period 2004–2006 on different core configurations. In that period the reactor operation was exclusively in subcritical conditions, with the exception of the critical reference core assessment at the beginning of the campaign where the maximum power was 80 W. In this work we'll focus on some selected RACE-T campaign outcomes:

- Characterization of the critical phase performed by fission rate traverses.
- Evaluation of the applicability of various experimental techniques for assessing a subcritical level. Those techniques are based on:

  a) The system response to a pulsed neutron source, in particular the Area-ratio method obtained by a D-T generator.
  b) The system response to a Source Jerk (SJ), in particular the Inverse Kinetics (IK) method applied to a SJ obtained by a D-T generator (the difference between SJ results by D-T generator and Cf-252 sources are analysed in [3]).
  c) The Source Multiplication technique.

By means of the methods mentioned above, reactivity estimates were performed at different core locations and for three different "clean" (control rods withdrawn) subcritical core configurations, namely SC0 (~ -500 pcm), SC2 (~ -2500 pcm) and SC3 (~ -5000 pcm).

II. SUBCRITICAL LEVEL MEASUREMENTS: THEORETICAL OUTLINES

II.A. The Area Method

Pulsed Neutron Source (PNS) Area methods are based on the analysis of the responses shown by a subcritical system to an external source pulse. A typical response of this kind is shown in Fig. 1, where the contributions of prompt and delayed neutrons are evidenced.

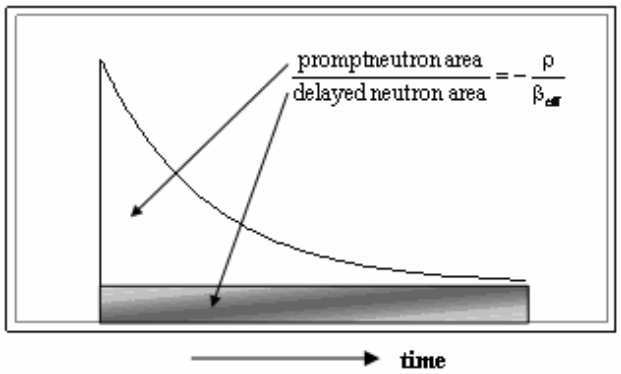

Fig. 1: Response shown by a subcritical system to an external source pulse.

In particular, the fundamentals of the Area-ratio method[4] consist in the evaluation of the absolute level of reactivity (in dollars) by measuring, independently by the detector position, the ratio between the area under the prompt peak and the delayed one after the injection of a neutron pulse in the subcritical system:

$$-\rho_{\$} = \frac{\text{Prompt neutron area}}{\text{Delayed neutron area}} = \frac{I_p}{I_t - I_p} \qquad (1)$$

where the prompt area I_p is proportional to the detector response without delayed neutron precursors and the delayed area Id is equal to the difference between the total area It and the prompt one. If the system response cannot be approximated by point kinetics, the reactivity value can apparently depend on the detector position r_D, and we will obtain, in place of Eq. (1), relationships like:

$$-\rho_{\$}(\mathbf{r}_D) = \frac{\text{Local prompt neutron area}}{\text{Local delayed neutron area}} = \frac{I_p(\mathbf{r}_D)}{I_t(\mathbf{r}_D) - I_p(\mathbf{r}_D)} \qquad (2)$$

In such cases, these spatial effects can be taken into account by calculating spatial correction factors obtained by

- Equivalent steady state methods obtained by solving time-independent inhomogeneous transport problems (see for example[5] for an application to the MUSE-4 case).
- Explicit time dependent analysis where time-dependent inhomogeneous transport problems are solved

II.A.1. Equivalent steady state methods

Consider the neutron source represented by $Q(\mathbf{r},E,\mathbf{\Omega},t)=Q(\mathbf{r},E,\mathbf{\Omega},t)\delta_+(t)$ and the signal due to the prompt neutrons alone; the prompt neutron flux $\Phi_p(\mathbf{r},E,\mathbf{\Omega},t)$ will obey to the prompt time-dependent ordinary transport equation, with the usual free-surface boundary conditions and the initial condition $\Phi_p(\mathbf{r},E,\mathbf{\Omega},0)=0$. Integrating from t=0 to t=∞, and defining the time integrated prompt neutron flux as

$$\tilde{\Phi}_p(\mathbf{r},\mathbf{\Omega},E) = \int_0^\infty \Phi_p(\mathbf{r},\mathbf{\Omega},E,t)dt \quad , \quad \tilde{\Phi}_p \text{ will}$$

satisfy the inhomogeneous (with external source) time-independent prompt transport equation with the initial condition and the condition $\lim_{t\to\infty}\Phi_p = 0$ (because the system is subcritical):

$$\mathbf{\Omega}\cdot\nabla\tilde{\Phi}_p + \Sigma_t\tilde{\Phi}_p = \langle\Sigma_{ins}\tilde{\Phi}_p\rangle + \left(\chi - \sum_i \beta_i\chi_d^i\right)\langle\nu\Sigma_f\tilde{\Phi}_p\rangle + Q(\mathbf{r},E,\mathbf{\Omega})$$

where β_i and χ_d^i are, respectively, the delayed neutron fraction and the delayed energy spectrum for each precursor group i, and χ is the total (prompt + delayed) spectrum. Σ_{ins} is the in-scattering cross section and, as usual, <> denotes integration. Analogously, the total time-integrated flux $\tilde{\Phi}(\mathbf{r},\mathbf{\Omega},E)$ can be defined by integrating the transport equation over time; $\tilde{\Phi}$ will then satisfy the inhomogeneous ordinary time-independent transport equation:

$$\mathbf{\Omega}\cdot\nabla\tilde{\Phi} + \Sigma_t\tilde{\Phi} = \langle\Sigma_{ins}\tilde{\Phi}\rangle + \chi\langle\nu\Sigma_f\tilde{\Phi}\rangle + Q(\mathbf{r},E,\mathbf{\Omega})$$

Therefore, the reactivity level of the system given by Eq. (2) can be evaluated by means of a steady state Monte Carlo or deterministic multigroup methods. In particular, being σ_D the detector cross section, we can write:

$$\frac{I_p(r_D)}{I_d(r_D)} = \frac{\iiint \sigma_D(r - r_D,\ E)\tilde{\Phi}_p dV\, dE\, d\Omega}{\iiint \sigma_D(r - r_D,\ E)\left(\tilde{\Phi} - \tilde{\Phi}_p\right) dV\, dE\, d\Omega}$$

II.A.2. Explicit time dependent analysis

Explicit time dependent analysis by numerical solution of the time-dependent inhomogeneous transport problems is the direct way to evaluate spatial correction factors for the Area-ratio method. In any case, also for these methods we have probably to devise some stratagems to evaluate, a priori, the delayed background shown in Fig. 1, without the need to run (useless?) multi-pulse CPU time-consuming cases in order to obtain a sufficient increase of the delayed background. Of course, it is of great interest to have explicit time dependent calculations in order to compare these results with those obtained by equivalent steady state methods.

II.B. INVERSE KINETICS APPLIED TO A SOURCE JERK

The inverse kinetics method is a widely known method used to analyse transient behaviour of reactor

systems. It is based on the inversion of the points kinetics equations which gives the reactivity versus time:

$$\rho_{\$} = 1 - \frac{\Lambda}{\beta_{eff}} \cdot \frac{S_d(t) + S_{eff} - \frac{dn}{dt}}{n(t)}$$

with the delayed neutron source equal to $S_d(t)=\Sigma_i\lambda_i C_i(t)$. The delayed neutron precursors group concentrations Ci(t) are calculated using the measured flux n(t) and the effective source S_{eff} is adjusted so that the inferred reactivity is steady after the source jerk. Finally, the reactivity is obtained by averaging the reactivity on an appropriate time range after the source jerk. This method will be referred in the following as SJ-Gen technique.

II.C. The Source Multiplication technique

II.C.1. MSA approximation

Let us consider a reference subcritical state characterized by a negative reactivity level ρ0 experimentally obtained by an independent method like a rod-drop measurement, and a generic subcritical core state i characterized by the reactivity ρi, assuming both states driven by the same external neutron source. If we measure for both states some counting rates T in a given core position r, the experimental reactivity for the state i will be given by:

$$\rho_i^{exp} = \rho_0^{exp} \cdot \frac{T_0^{exp}(\mathbf{r})}{T_i^{exp}(\mathbf{r})} \equiv \rho_i^{MSA} \quad (1)$$

This is the so-called MSA approximation (from the French Multiplication Source Approchée), which presumes that the ratio $T_0(\mathbf{r})/T_1(\mathbf{r})$ does not depend on the position **r**.

II.C.2. MSM correction

If the above listed MSA hypotheses break we need for (calculated) correction factors. We can write for the reference state:

$$\rho_0 \cdot T_0(\mathbf{r}) = - < \phi_0^* \mathbf{S} > \cdot \frac{T_0(\mathbf{r})}{< \phi_0^* \mathbf{F}_0 \psi_0 >} \equiv -S_{eff,0} \cdot \varepsilon_0(\mathbf{r}) \quad (2)$$

were $S_{eff,0}$ and $\varepsilon_0(\mathbf{r})$ denote, respectively, the effective source and the detector efficiency (at position **r**) for the state 0, and ϕ_0^* is the associated adjoint homogeneous flux solution. Analogously we can write for the generic subcritical state i:

$$\rho_i \cdot T_i(\mathbf{r}) = - < \phi_i^* \mathbf{S} > \cdot \frac{T_i(\mathbf{r})}{< \phi_i^* \mathbf{F}_i \psi_i >} \equiv -S_{eff,i} \cdot \varepsilon_i(\mathbf{r}) \quad (3)$$

From (4) and (5) we obtain:

$$\frac{\rho_i \cdot T_i(\mathbf{r})}{\rho_0 \cdot T_0(\mathbf{r})} = \frac{S_{eff,i} \cdot \varepsilon_i(\mathbf{r})}{S_{eff,0} \cdot \varepsilon_0(\mathbf{r})} \quad (4)$$

By comparison with Eq. (3) we see that the MSA approximation is equivalent to assume that effective source and detector efficiency remain unchanged when passing from state 0 to state i. Eq. (6) must be evaluated by calculation, and we have to impose that:

$$\frac{\rho_i^{exp} \cdot T_i^{exp}(\mathbf{r})}{\rho_0^{exp} \cdot T_0^{exp}(\mathbf{r})} = \frac{\rho_i^{cal} \cdot T_i^{cal}(\mathbf{r})}{\rho_0^{cal} \cdot T_0^{cal}(\mathbf{r})}$$

Thus, we have to replace the MSA formulation (3) with the modified formulation:

$$\rho_i^{exp} = \left(\rho_0^{exp} \cdot \frac{T_0^{exp}(\mathbf{r})}{T_i^{exp}(\mathbf{r})} \right) \cdot \left(\frac{\rho_i^{cal} \cdot T_i^{cal}(\mathbf{r})}{\rho_0^{cal} \cdot T_0^{cal}(\mathbf{r})} \right) \equiv \rho_i^{MSA} \cdot MSM_{i \to 0}^{cal}(\mathbf{r})$$

The last term, the correction factors, depending on the position, have to be evaluated by calculation. This is the so-called MSM method (Modified Source Multiplication) which takes into account spatial and energetic effects, due to type and position of the detector.

III. EXPERIMENTAL SETUP

III.A. Description of the TRIGA reactor

The RC-1 TRIGA reactor, located at the ENEA Casaccia research centre nearby Rome, is a 1 MW Mark II reactor built in 1960. It is a light-water reactor cooled by natural convection, with a 284-mm-thick annular graphite reflector. The core has a 565-mm-diameter cylindrical configuration with 127 locations that are arranged in seven concentric rings, namely A, B, C, D, E, F and G (see Figs. 2 and 6). Each location can be filled with either a fuel element or some other component like graphite rods, a neutron source or a measurement channel. The stainless-steel-clad fuel material with 37.3-mm diameter and 381-mm height is a homogeneous mixture of uranium and zirconium hydride terminated at both the bottom and top by 87.5-mm-high cylindrical graphite slugs that act as axial reflectors. There are four boron-carbide control rods: two fuel-follower shim rods (SH1 and SH2), one fuel-follower safety rod (SEC) and one regulating rod (REG), not fuel followed.

The fuel elements consist of a stainless steel clad (AISI-304, 0.05 cm thick, 7.5 g/cm^3 density) characterized by an external diameter of 3.73 cm and a total height of 72 cm end cap included (Fig. 2.c). The fuel is a cylinder (38.11 cm high, 3.63 cm external diameter, 5.9 g/cm^3 theoretical density) of a ternary alloy uranium-zirconium-hydrogen (H-to-Zr atom ratio is 1.7 to 1; the uranium, enriched to 20% in U-235, makes up 8.5% of the mixture by weight: the total uranium content of a rod, on the average, is 197 g, of which 39 g is fissile) with a metallic zirconium rod inside (38.11 cm high, 0.5 cm in diameter, 6.49 g/cm^3 of density). There are two graphite cylinders (8.7 cm high, 3.63 cm in diameter, 2.25 g/cm^3 of density) at the top and bottom of the fuel rod. Externally two end-fittings are present in order to allow the remote movements and the correct locking to the grid.

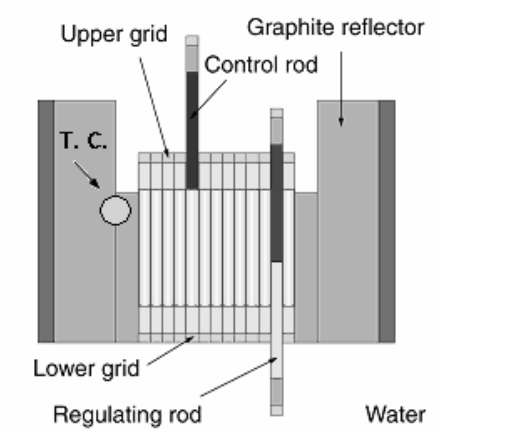

Fig. 2.a TRIGA reactor core, reflector and control rod positions (Side view).

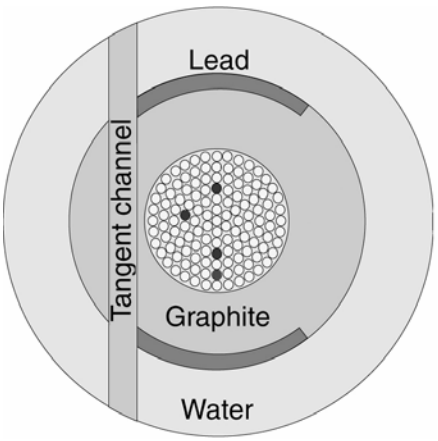

Fig. 2.b TRIGA reactor core, reflector and control rod positions (Radial view).

Fig. 2.c TRIGA fuel element.

III.B. Neutron sources

For the subcritical configurations, the reactor was coupled with the following neutron sources.

- A pulsed deuterium-tritium neutron generator, accelerating deuterium ions onto a tritium target, and producing 14.1-MeV-neutron bursts with strength 2.10^8 neutrons/s at maximal frequency. The frequency range spanned from 1 to 50 Hz. The pulse duration was less than 1 μs. The neutron generator was located at the core center A01.
- A Cf-252 source, with a strength of 0.4 Ci, was used to perform Source Multiplication experiments using a Fast Rabbit (FR) location in the B02 position in ring B (Fig. 6).

III.C. Instrumentation

For the characterization of the critical phase by fission rate traverses, a special fuel pin was used. This fuel is hollowed in the centre, and enables the fission chamber to be inserted inside the fuel. The hole has a diameter of 5 mm, allowing the insertion of the Ø1.5 mm fission chambers. The cross section of this special pin is shown in Fig. 3.

The position of the fission chamber in the special fuel pin corresponds to the mid plane of the core. A tight tube is fixed at the end of fuel and enables the connexion cable to leave the pool of the reactor. Before each measurement, one withdraws a fuel pin and replaces it by the special fuel pin.

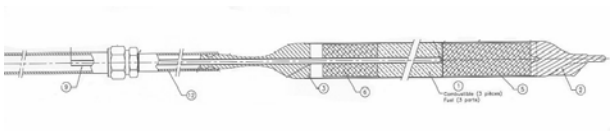

Fig. 3: Cross-section of the special fuel pin.

For the evaluation of the applicability of various experimental techniques for assessing a subcritical level, the instrumentation consisted of fission chambers (labelled from A to D in Fig. 6), current-sensitive amplifiers and the X-MODE data acquisition system[1]. The fission chambers were placed within the core region close to the reflector (see Fig. 6). The main purpose of X-MODE is to integrate in a single system all the features needed for reactor measurements. The main asset of X-MODE is an accurate time stamping capability that offers many methods of investigating acquired data.

IV. FISSION RATES MEASUREMENTS

Radial traverses enable one to analyse the shape of the fission rate in different energy ranges, and to look at

possible asymmetry effects. Measurements were carried out for the reference critical configuration shown in Fig. 4, along the main G13-G31 diagonal (Fig. 4), in the positions G13, F11, E09, D07, C05, C11, D16, E21, F26 and G31. The measurements were performed in critical condition with a reactor power in the range 10÷80 W.
In order to cover the broadest range in energy, various types of deposits were used:

- Two U-235 fission chambers (n°1847 and n°331) for thermal fission rates.
- One Np-237 fission chamber (n°1523) for intermediate spectrum range.
- One U-238 fission chamber (n°861) for the fast energy range.

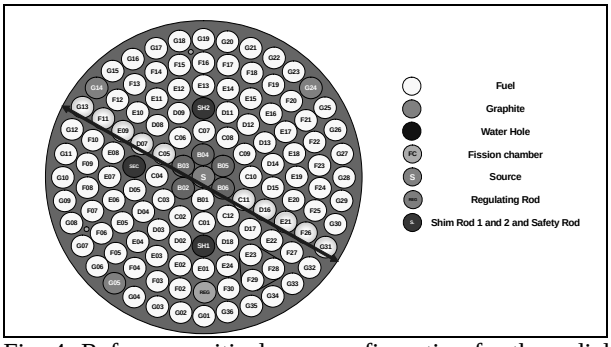

Fig. 4: Reference critical core configuration for the radial fission rates measurement.

The results relative to the G13-G31 diagonal are plotted in Fig. 5 for each fission chamber.

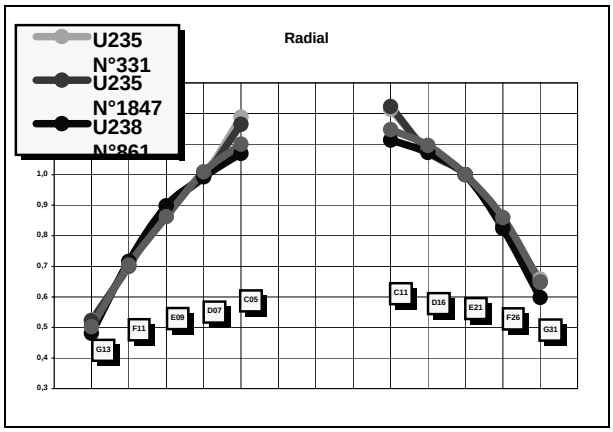

Fig- 5: Normalized count rates on G13-G31 diagonal.

The effect of the asymmetry shown in Fig. 5 is due to the presence of the tangential beam tube of important diameter situated near the core mid-plane, in the reflector (cf. Fig. 2). This tube removes an important part of the water and induces a very important local void effect.

V. Subcritical level measurements

V.A. Core configurations

The investigated core configurations, all characterised by main control rods withdrawn, are the following: one reference critical configuration (REF), the REF configuration with the regulation rod down (representing the reference subcritical configuration for the Source Multiplication method) and three subcritical configurations, namely SC0 (~ -500 pcm), SC2 (~ -2500 pcm) and SC3 (~ -5000 pcm), as shown in Fig. 6. The fission chambers, the Fast Rabbit (FR) pipe and the neutron generator were always placed in-core during the experimental campaign. It should be mentioned that the REF core configuration was critical with the regulating rod (REG) 51% inserted (cf. Figs. 2 and 6).

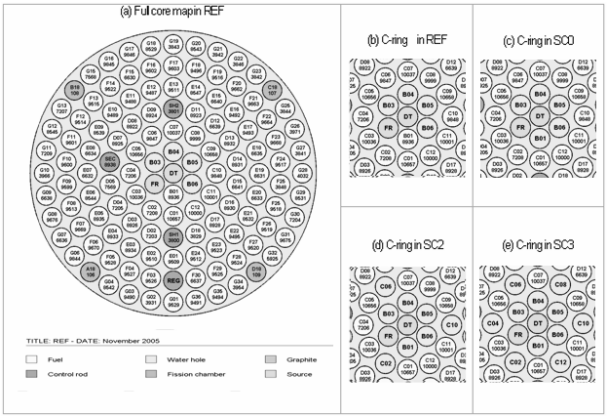

Fig. 6: Core configurations for the subcritical level analyses. One removes three fuel elements in C-ring to shift from one subcritical configuration to another. The Fast Rabbit (FR) pipe is in B02 and the neutron generator (DT) in A0.

V.B. Experimental results and data analysis

The following methods have been into account for the inter-comparison: the Area-ratio technique (PNS-Area), the Inverse Kinetics-Source Jerk technique based on the transient caused by the neutron generator shutdown (SJ-Gen) and the Approximated Source Multiplication technique (MSA).

All the reactivity estimates for the three subcritical configurations are displayed in Fig. 7. For SC0, the uncertainties are about 1% for the PNS-Area technique, 3.1% for the MSA technique, 4.0% to 4.4% for the SJ-Gen technique. For SC2, the uncertainties are about 0.4% for the PNS-Area technique, 3.1% for the MSA technique, 6% to 7% for the SJ-Gen technique. For SC3, the uncertainties are about 0.5% for the PNS-Area

technique, 3.1% for the MSA technique, 5% to 6.5% for the SJ-Gen technique.

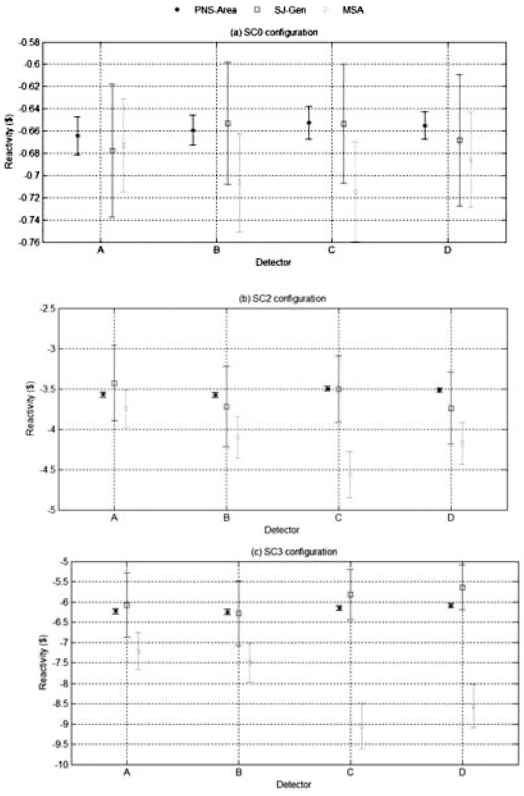

Fig. 7: Comparison between PNS, SJ-Gen and MSA techniques with all rods up. *The error bars corresponds to a confidence level of 95% (1$~700 pcm)*

First, it appears that the PNS-Area and SJ-Gen reactivity estimates are always equal with a confidence level of 95%. Second, the MSA technique is clearly the most detector location dependent. The discrepancies from the PNS-Area estimates are about 1%-5% for SC0, 5%-19% for SC2 and 16%-40% for SC3. Conversely, the PNS-Area technique is the least detector location dependent with a spread of 1.22% at most for SC3.

VI. CONCLUSIONS

To have at one's disposal a reference critical state, contrary to the foreseen situations in ADS, allows the inter-comparison of dynamic methods to measure the subcritical level (PNS Area-ratio, Source Jerk) with the static method MSA, which is usually taken as reference but requires for large MSM spatial correction factors at deep sub-criticalities.

Under this point of view, the RACE-T experiments have allowed the testing of different techniques to measure the subcritical level in ADS. Coherently with the outcomes from MUSE, the PNS Area-ratio method seems to be the most stable for what concerns the spatial effects, even if such stability has to be supported by theoretical and numerical confirmations.

For what concerns the Inverse Kinetics/Source Jerk technique, the measurements provided reactivity estimates always in excellent agreement with those obtained by the Area-ratio technique, although a discrepancy between PNS Area-ratio and Inverse Kinetics/Source Jerk results can be clearly be observed when increasing the subcriticality level.

VII. MULTI-PURPOSE DATA ACQUISITION SYSTEM

The main purpose of X-MODE is to integrate in a single system all features needed for reactor measurements. It will also provide tools to improve data processing such as online treatments and data reduction algorithms. It is noteworthy that the great asset of X-MODE is a precise time marking capability, which is a powerful way of investigating acquired data. Time marking acts as a triggerless acquisition mode in which each event detected is counted and marked, as a result that the maximum information on the experiment is stored. In other words, data processing is not limited by the acquisition settings. Such a triggerless system is widespread in the field of particle physics and has previously been used in nuclear noise measurements. Nowadays, thanks to the improvements of storage capabilities, it can be useful in a great number of measurements.

ACKNOWLEDGMENTS

The authors appreciate the efforts and support of all the scientists and institutions involved in EUROTRANS and the presented work, as well as the financial support of the European Commission through the contract FI6W-CT-2004-516520.

REFERENCES

1. Word's Equation Editor, Microsoft Word.
2. M. P. BROWN and K. AUSTIN, *Title of Book*, pp. 25–30, J. SMITH, Ed., Publisher Name, Publisher City, Publisher State (2004).
3. M. P. BROWN and K. AUSTIN, "With or Without Title of Paper," *Title of Journal*, **36**, 102 (2004).
4. R. T. WANG, "Title of Paper," *Proc. Title*, Location of Meeting, Date of Meeting, Vol. No., p. No., Pub lisher of Proceedings (2004).
5. J. U. Knebel et al., "IP EUROTRANS: a European research programme for the transmutation of high-level nuclear waste in an accelerator-driven system",

8th Information Exchange Meeting on Actinide and Fission Product Partitioning &Transmutation, Las Vegas, Nevada, USA (2004).
6. G. Imel et al., "The TRADE experiment and progress", GLOBAL 2003, New Orleans, Louisiana, USA (2003).
7. C. Jammes et al., "Absolute Reactivity Calibration of Accelerator-Driven Systems after RACE-T Experiments ", PHYSOR-2006**,** Vancouver, BC, Canada (2006).
9. N.J. Sjöstrand, Arckiv. Fis. 11, 233 (1956), see also in G.I. Bell and S. Glasstone, 'Nuclear Reactor Theory', (pp.546-549), 1970, Van Nostrand Reinhold Company.
10. M. Carta et al, "Reactivity Assessment and Spatial Time-Effects from the MUSE Kinetics Experiments", PHYSOR-2004, Chicago, IL USA (2004).
11. B. Geslot et al., "Multimode Acquisition System Dedicated to Experimental Neutronic Physics", IMTC 2005, Ottawa, Canada